Biointerface Research in Applied Chemistry
Open-Access Journal (ISSN: 2069-5837)

Article
Volume 13, Issue 5, 2023, 434
https://doi.org/10.33263/BRIAC135.434

A Titanium-Enhanced Boron Nitride Fullerene for the Drug Delivery of 5-Fluorouracil Anticancer: DFT Study

Muhammad Da'i [1,*], Erindyah Retno Wikantyasning [1], Maryati [1], Arifah Sri Wahyuni [1], Mahmoud Mirzaei [2,*]

[1] Faculty of Pharmacy, Universitas Muhammadiyah Surakarta, Surakarta, Indonesia; muhammad.dai@ums.ac.id (M.D.); erindyah.rw@ums.ac.id (E.R.W.); maryati@ums.ac.id (M.); arifah.wahyuni@ums.ac.id (A.S.W.);
[2] Child Growth and Development Research Center, Research Institute for Primordial Prevention of Non-Communicable Disease, Isfahan University of Medical Sciences, Isfahan, Iran; mirzaei.res@gmail.com (M.M.);
* Correspondence: muhammad.dai@ums.ac.id (M.D.); mirzaei.res@gmail.com (M.M.);

Scopus Author ID 57189357187 (M.D.)
13204227300 (M.M.)

Received: 27.09.2022; Accepted: 30.10.2022; Published: 19.12.2022

Abstract: Benefits of employing titanium (Ti)-enhanced boron nitride (BN) fullerene for the drug delivery of 5-fluorouracil (5FU) anticancer were investigated in this work by performing density functional theory (DFT) calculations. The models were optimized to obtain their stabilized geometries of singular states to be combined with each other to obtain the complex model of the bimolecular state. Six complexes of 5FU@TiBN models were obtained based on their stabilized interacting configuration with different electronic molecular orbital features and adsorption strength. C…Ti, O…Ti, F…Ti, and H…B types of interaction were found for the formation of complexes. Their details were examined by the evaluated features of the quantum theory of atoms in molecules (QTAIM) analyses. Based on the achievements, the models of 5FU@TiBN complexes were found suitable regarding the meaningful values of adsorption strength. However, the models of relaxed configurations showed significant impacts on both the complexes' structural and electronic features. Additionally, measuring variations of such electronic molecular orbital features could be a tool for complex recognition. In this regard, the investigated 5FU@TiBN complexes could be proposed for initiating a drug delivery process by specifying the desired configuration for approaching the purpose for the case of employing the TiBN adsorbent towards the 5FU anticancer.

Keywords: boron nitride; fullerene; 5-fluorouracil; anticancer; drug delivery; DFT.

1. Introduction

Boron nitride (BN) nanostructures with the combination of boron and nitrogen atoms were found after the pioneering innovation of carbon nanostructures [1]. The models were found even at higher suitability for substituting carbon nanostructures in many applications, especially in the cases of interactions and adsorptions [2]. Similar to the carbon nanostructures, various geometrical architectures of BN nanostructures, such as tubular, planar, conical, and spherical, have been found up to now [3-6]. Furthermore, the heteroatomic composition of BN nanostructures could increase the tendency of their surface to participate in molecular communications in better modes than carbon nanostructures [7]. Accordingly, earlier efforts indicated a significant adsorbent role for the BN nanostructures for adsorbing other molecular and atomic substances [8-10].

Additionally, inserting atomic dopants could create a specific region of interactions to enhance BN nanostructures' function for conducting more efficient adsorption processes [11-13]. To this aim, metal atoms have been seen as a useful dopant for enhancing the features of nanostructures for approaching desired functions [14-16]. In this regard, a model of BN fullerene nanostructure was investigated in this work by an enhancement of titanium (Ti) dopant for adsorbing a known anticancer drug, 5-fluorouracil (5FU). It is worth mentioning that Ti-related compounds are known for employing them in medical applications [17]. The stoichiometry formula of the TiBN model is $TiB_{11}N_{11}$, in which its stabilized geometry was found by performing density functional theory (DFT) calculations. The stoichiometry formula of the 5FU model is $C_4H_3FN_2O_2$, in which its geometry was also stabilized by performing DFT calculations. Next, molecular combinations of 5FU and TiBN were explored by performing additional calculations to yield the stabilized interacting bimolecular models. The models of 5FU, TiBN, and 5FU@TiBN are shown in Figure 1. Indeed, these examinations were done to learn the benefits of employing the Ti-enhanced BN fullerene for adsorbing the 5FU anticancer substance for initiating a drug delivery process.

It is known that cancer patients have serious difficulties dealing with the current anticancers and several efforts have been done for enhancing the efficacy and reducing the adverse effects of anticancers to this time [18-20]. On the other hand, 5FU has been a very useful anticancer drug for years, and its adverse effects restrict it from showing an efficient treatment [21]. To this time, considerable efforts have been dedicated to improving efficiency of 5FU for approaching a better therapeutic treatment [22-24]. Initiating a nano-based targeted drug delivery platform is among the proposed protocols for approaching better results about therapeutic activities [25-27]. In this regard, details of interactions between nanostructures and drug substances should be known to find suitable adsorbents for working in the drug delivery platform [28]. Hence, the current work was done to analyze an enhanced model of nanostructure (TiBN) toward adsorbing a representative anticancer drug (5FU). The results of earlier works affirmed the hypothesis of employing nanostructures for adsorbing 5FU [29-31], and details of such an adsorption process by means of TiBN were investigated in the current work. To learn such details, using computational chemistry tools is helpful in recognizing the materials at the smallest molecular and atomic scales [32-37]. Accordingly, the models of this work were investigated based on the computer-based stabilized geometries and evaluated descriptors as exhibited in Figure 1 and Table 1.

2. Materials and Methods

As shown in Figure 1, the investigated models of this work, including singular TiBN and 5FU molecule and bimolecular 5FU@TiBN complexes, were visualized using the ChemCraft program [38]. All exhibited models were optimized to find their stabilized geometries using the wB97XD/6-31G* level of DFT calculations as implemented in the Gaussian program [39]. Before optimizing the bimolecular complexes, singular models were optimized, and they were combined with being inserted in re-optimization calculations to find the stabilized geometries of complexes. To investigate energies of bimolecular complexes, the impacts of basis set superposition error (BSSE) were examined [40]. Additionally, quantum theories of atoms in molecules (QTAIM) were analyzed using the MultiWfn program to detect involving interactions in the bimolecular complexes [41, 42]. As a result of optimization calculations, six configurations were found for 5FU@TiBN bimolecular complexes, as indicated by C1 to C6 in Figure 1. Additionally, related descriptors, including frontier

molecular orbital energy levels of the highest occupied and the lowest unoccupied molecular orbitals (HOMO and LUMO), energy gap (GAP), adsorption energy (ADS), and QTAIM features, were summarized in Table 1. INT, DIS, ρ, $\nabla^2\rho$, and H, implied for interaction types, distances, the density of all electrons, Laplacian of electron density, and energy density, respectively.

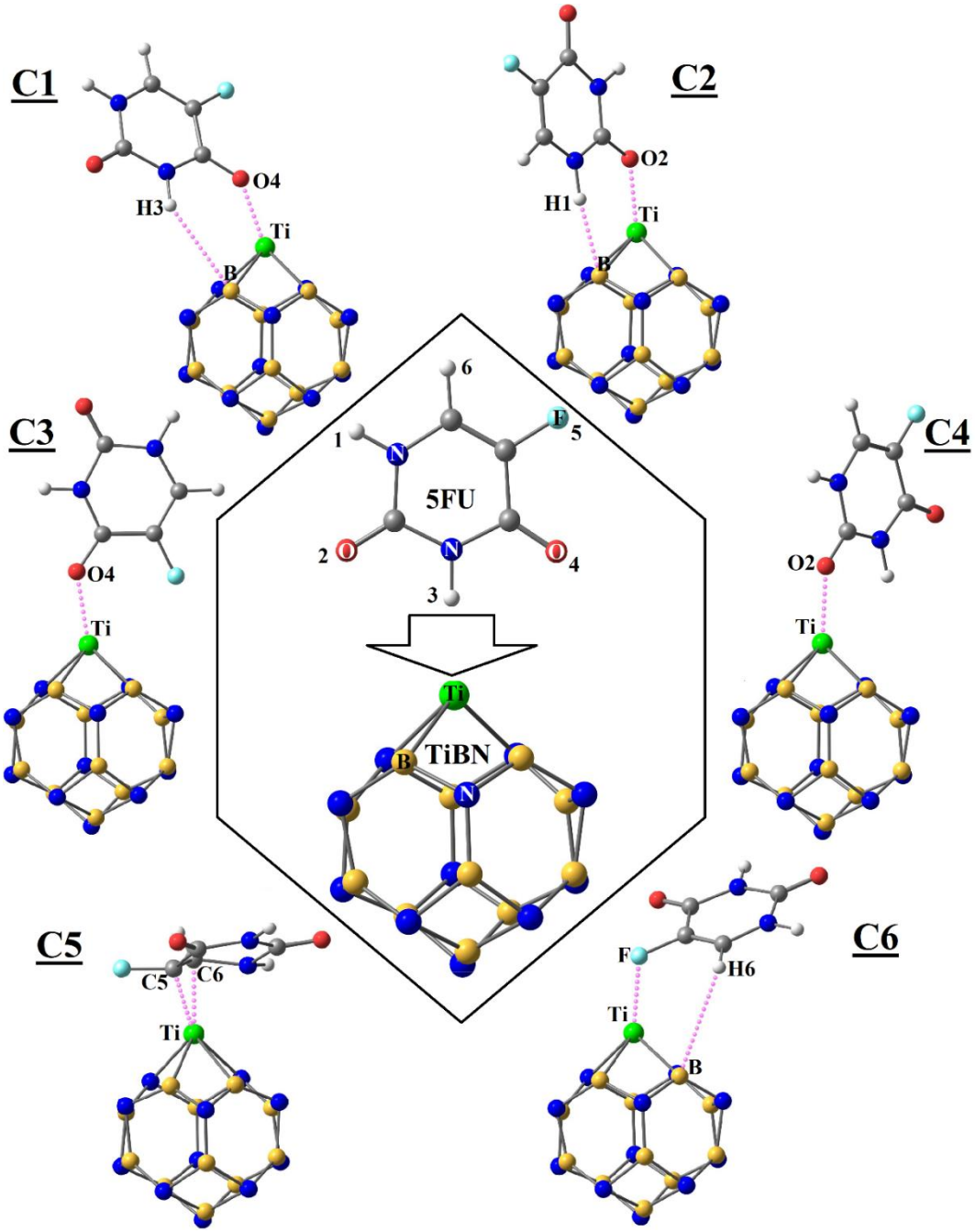

Figure 1. The stabilized models of 5FU, TiBN, and C1-C6 of 5FU@TiBN complexes.

3. Results and Discussion

The main goal of this work was to investigate the benefits of employing a Ti-enhanced BN (TiBN) fullerene for the drug delivery of 5FU anticancer. Indeed, the goal of this work was followed in accordance with the importance of developing efficient applications of nanostructures for biological related systems [43-45]. Nanostructures have been always expected to work in various aspects of drug delivery processes such as drug carriers and sensors; however, the topic has been still under investigations and developments [46-50]. The

investigated singular models and their related bimolecular complexes through performing DFT calculations are exhibited in Figure 1. The models were optimized to obtain their stabilized geometries for further discussion of the goal of this work. For the state of bimolecular models, not only one 5FU@TiBN model but six configurations were obtained based on various routes of interactions between 5FU and TiBN substances. Because of the different atomic sites of the 5FU molecule, different possibilities of interactions with the TiBN substance were examined, resulting in six optimized configurations of bimolecular models. The evaluated descriptors of all models are summarized in Table 1.

Table 1. Evaluated descriptors for the investigated models.[1]

Model	**TiBN**	**5FU**	**C1**	**C2**	**C3**	**C4**	**C5**	**C6**
HOMO eV	-5.582	-6.786	-4.922	-5.407	-4.639	-4.841	-6.243	-5.307
LUMO eV	-2.970	-1.378	-3.385	-2.578	-3.476	-2.903	-3.119	-2.712
GAP eV	2.612	5.408	1.537	2.829	1.163	1.938	3.123	2.594
ADS eV	–	–	-1.735	-1.979	-1.775	-1.726	-1.439	-0.926
INT1:	–	–	O…Ti	O…Ti	O…Ti	O…Ti	C…Ti	F…Ti
DIS Å	–	–	2.043	2.021	2.059	2.064	2.175	2.141
ρ au	–	–	0.073	0.074	0.065	0.064	0.081	0.048
$\nabla^2\rho$ au	–	–	0.411	0.447	0.406	0.396	0.138	0.298
H au	–	–	-0.005	-0.006	-0.009	-0.008	-0.016	-0.007
INT2:	–	–	H…B	H…B	–	–	C…Ti	H…B
DIS Å	–	–	2.932	2.171	–	–	2.047	3.159
ρ au	–	–	0.007	0.029	–	–	0.107	0.005
$\nabla^2\rho$ au	–	–	0.017	0.032	–	–	0.175	0.013
H au	–	–	-0.001	-0.004	–	–	-0.035	-0.001

[1]The models are shown in Figure 1.

C1 and C2 are two configurations of 5FU@TiBN bimolecular models with contributions of two types of O…Ti and H…B interactions. Both models were stabilized, and their geometries were found, as shown in Figure 1. It should be mentioned that different positions of 5FU were involved in interactions with the Ti-region of TiBN substance, in which O4 and H3 were for C1 and O2 and H1 were for C2. Accordingly, different values of descriptors were evaluated for the mentioned models. Examining the values of HOMO and LUMO could show different electronic molecular orbital features for the models with a higher similarity of C2 to the singular TiBN compared to that of C1. The evaluated values of GAP were 1.537 eV for C1 and 2.829 eV for C2 versus 2.612 eV for the singular TiBN, showing that mentioned similarity. The exact energy levels of HOMO and LUMO were in agreement with the similarity of GAP values. This achievement could imply a significant role of the TiBN substance in adsorbing the 5FU substance to manage the whole adsorption process. For examining the strength of adsorption of 5FU by the TiBN substance, energy differences of bimolecular and singular counterparts were compared to evaluate the values of ADS. In this regard, C1 showed a value of -1.735 eV, and C2 showed a value of -1.979 eV, revealing a higher strength of adsorption for C2 than C1. Further analyses of interactions indicated higher levels of contributions of both of O…Ti and H…B to the interactions in C2 in comparison with C1. Besides the obtained relaxation of C2 substances at a closer distance to each other, the evaluated QTAIM features showed a higher suitability of electronic portions of the interactions of C2 rather than those of C1. As a consequence, formations of C1 and C2 were found achievable with higher suitability for C2.

C3 and C4 are the complexes with the optimized configurations of 5FU@TiBN in the interaction routes of O4…Ti and O2…Ti, respectively. It is worth mentioning that the Ti-region was dominant in conducting the adsorption processes, in which it was significantly involved in interactions of all 5FU@TiBN complexes. A smaller value of GAP was found for

C3 (1.163 eV) in comparison with that of C4 (1.938 eV). Accordingly, energy values of HOMO and LUMO levels were changed in C3 and C4 bedsides compared with the singular TiBN. More or less significant discrepancies were observed for the molecular orbital levels of complexes and singular models. Based on the evaluated values of ADS, C3 (-1.775 eV) was found at a higher adsorption strength than C4 (-1.726 eV). The evaluated QTAIM features also affirmed such a higher level of strength for C3 than for C4. Comparing the obtained strengths of C3 and C4 with each of C1 and C2 could reveal an order of C2 > C3 > C1 > C4 for the models up to now.

C5 is the obtained complex with an optimized configuration through two C…Ti interactions between 5FU and TiBN substances. As shown in Figure 1, the adsorbed 5FU substance was indeed perpendicular to the TiBN substance, different from the configurations of other complexes. The evaluated molecular orbital features indicated a significant discrepancy of values from the changes of other complexes. A wider GAP (3.123 eV) was found for C5 compared with other complexes and even the singular TiBN. The evaluated strength of adsorption (-1.439 eV) was meaningful but lower than those of C1 to C4. Details of interactions also indicated electronic portions of interactions for the involved C…Ti types. The last obtained complex is C6 with an optimized configuration of F…Ti and H…B interactions. This model was indeed at the lowest level of adsorption strength (-0.926 eV) but still meaningful. Accordingly, the models were ordered as C2 > C3 > C1 > C4 > C5 > C6 regarding the adsorption strengths. By the evaluated QTAIM features, both of F…Ti and H…B types of C6 were weak interactions, and the obtained complex was placed at the weakest level compared to the available complexes.

4. Conclusions

Based on the obtained results, some achievements could be summarized regarding the goal of this work to study the benefits of employing the TiBN substance for the drug delivery of 5FU anticancer. The first achievement could be mentioned by the obtained optimized configurations of 5FU@TiBN complexes, in which six different configurations were found. The second achievement could be focused on showing the significant role of the Ti-region in conducting the adsorption process, in which 5FU was in interaction with this region in all complexes. The third achievement could be referred to as the observed variations of molecular orbital features of complexes and singular models to provide a possibility of an electronic-based diagnosis of complex formations. The strength of adsorption could be laced at the fourth achievement, in which all complexes were in reasonable levels of strength but with different magnitudes compared to each other. The fifth achievement could be summarized by the evaluated QTAIM features showing the electronic portions of interactions for the models. And as a final achievement, the obtained models of 5FU@TiBN complexes were found suitable for formation, and their features indicated their significant roles in initiating a drug delivery process of 5FU anticancer.

Funding

This research received no external funding.

Acknowledgments

This research has no acknowledgment.

Conflicts of Interest

The authors declare no conflict of interest.

References

1. Roy, S.; Zhang, X.; Puthirath, A.B.; Meiyazhagan, A.; Bhattacharyya, S.; Rahman, M.M.; et al. Structure, properties and applications of two-dimensional hexagonal boron nitride. *Advanced Materials* **2021,** *33,* 2101589, https://doi.org/10.1002/adma.202101589.
2. Yadav, A.; Dindorkar, S.S.; Ramisetti, S.B. Adsorption behaviour of boron nitride nanosheets towards the positive, negative and the neutral antibiotics: insights from first principle studies. *Journal of Water Process Engineering* **2022,** *46,* 102555, https://doi.org/10.1016/j.jwpe.2021.102555.
3. Farhami, N. A computational study of thiophene adsorption on boron nitride nanotube. *Journal of Applied Organometallic Chemistry* **2022,** *2,* 163, https://doi.org/10.22034/jaoc.2022.154821.
4. Stewart, J.C.; Fan, Y.; Danial, J.S.; Goetz, A.; Prasad, A.S.; Burton, O.J.; et al. Quantum emitter localization in layer-engineered hexagonal boron nitride. *ACS Nano* **2021,** *15,* 13591, https://doi.org/10.1021/acsnano.1c04467.
5. Wang, C.; Shen, L.; Wu, L. Adsorption and sensing of an anticancer drug on the boron nitride nanocones; a computational inspection. *Computer Methods in Biomechanics and Biomedical Engineering* **2021,** *24,* 151, https://doi.org/10.1080/10255842.2020.1815716.
6. Anafcheh, M. A comparison between density functional theory calculations and the additive schemes of polarizabilities of the Li-F-decorated BN cages. *Journal of Applied Organometallic Chemistry* **2021,** *1,* 125, https://doi.org/10.22034/jaoc.2021.292384.1027.
7. Liu, X.; Ahmadi, Z. H2O and H2S adsorption by assistance of a heterogeneous carbon-boron-nitrogen nanocage: computational study. *Main Group Chemistry* **2022,** *21,* 185, https://doi.org/10.3233/MGC-210113.
8. Bangari, R.S.; Yadav, A.; Sinha, N. Experimental and theoretical investigations of methyl orange adsorption using boron nitride nanosheets. *Soft Matter* **2021,** *17,* 2640, https://doi.org/10.1039/D1SM00048A.
9. Yadav, A.; Dindorkar, S.S.; Ramisetti, S.B.; Sinha, N. Simultaneous adsorption of methylene blue and arsenic on graphene, boron nitride and boron carbon nitride nanosheets: insights from molecular simulations. *Journal of Water Process Engineering* **2022,** *46,* 102653, https://doi.org/10.1016/j.jwpe.2022.102653.
10. Bibi, S.; Ur-Rehman, S.; Khalid, L.; Bhatti, I.A.; Bhatti, H.N.; Iqbal, J.; et al. Investigation of the adsorption properties of gemcitabine anticancer drug with metal-doped boron nitride fullerenes as a drug-delivery carrier: a DFT study. *RSC Advances* **2022,** *12,* 2873, https://doi.org/10.1039/D1RA09319C.
11. Mohammadi, M.D.; Abdullah, H.Y. Vinyl chloride adsorption onto the surface of pristine, Al-, and Ga-doped boron nitride nanotube: a DFT study. *Solid State Communications* **2021,** *337,* 114440, https://doi.org/10.1016/j.ssc.2021.114440.
12. Mohammadi, M.D.; Abdullah, H.Y. The adsorption of bromochlorodifluoromethane on pristine, Al, Ga, P, and As-doped boron nitride nanotubes: a study involving PBC-DFT, NBO analysis, and QTAIM. *Computational and Theoretical Chemistry* **2021,** *1193,* 113047, https://doi.org/10.1016/j.comptc.2020.113047.
13. Maleki, P.A.; Nemati-Kande, E.; Saray, A.A. Using quantum density functional theory methods to study the adsorption of fluorouracil drug on pristine and Al, Ga, P and As doped boron nitride nanosheets. *ChemistrySelect* **2021,** *6,* 6119, https://doi.org/10.1002/slct.202101333.
14. Yuksel, N.; Kose, A.; Fellah, M.F. A density functional theory study for adsorption and sensing of 5-fluorouracil on Ni-doped boron nitride nanotube. *Materials Science in Semiconductor Processing* **2022,** *137,* 106183, https://doi.org/10.1016/j.mssp.2021.106183.
15. Liu, F.; Zhou, Q.; Li, Y.; Pang, J. Cu-doped boron nitride nanosheets for solid-phase extraction and determination of rhodamine B in foods matrix. *Nanomaterials* **2022,** *12,* 318, https://doi.org/10.3390/nano12030318.
16. Behmanesh, A.; Salimi, F.; Ebrahimzadeh-Rajaei, G. Sensing of letrozole drug by pure and doped boron nitride nanoclusters: density functional theory calculation. *Pharmaceutical Sciences* **2022,** *in press,* https://doi.org/10.34172/PS.2022.35.
17. Froes, F.S. Titanium for medical and dental applications - an introduction. *Titanium in Medical and Dental Applications* **2018,** *3*, https://doi.org/10.1016/B978-0-12-812456-7.00001-9.

18. Rahib, L.; Wehner, M.R.; Matrisian, L.M.; Nead, K.T. Estimated projection of US cancer incidence and death to 2040. *JAMA Network Open* **2021,** *4,* e214708, https://doi.org/10.1001/jamanetworkopen.2021.4708.
19. Hudiyawati, D.; Syafitry, W. Effectiveness of physical and psychological treatment for cancer-related fatigue: systematic review. *Jurnal Kesehatan* **2021,** *14,* 195, https://doi.org/10.23917/jk.v14i2.15596.
20. Saroyo, H.; Saputri, N.F. Cytotoxicity of mangrove leaves (rhizophora) ethanolic extract on cancer cells. *Journal of Nutraceuticals and Herbal Medicine* **2021,** *4,* 43, https://doi.org/10.23917/jnhm.v4i1.15657.
21. Longley, D.B.; Harkin, D.P.; Johnston, P.G. 5-Fluorouracil: mechanisms of action and clinical strategies. *Nature Reviews Cancer* **2003,** *3,* 330, https://doi.org/10.1038/nrc1074.
22. Ramirez-Malule, H.; Cardona, G.W. Bibliometric analysis of recent research on 5-Fluorouracil (2015–2020). *Journal of Applied Pharmaceutical Science* **2022,** *12,* 70, http://dx.doi.org/10.7324/JAPS.2021.120106.
23. Sethy, C.; Kundu, C.N. 5-Fluorouracil (5-FU) resistance and the new strategy to enhance the sensitivity against cancer: implication of DNA repair inhibition. *Biomedicine & Pharmacotherapy* **2021,** *137,* 111285, https://doi.org/10.1016/j.biopha.2021.111285.
24. Azwar, S.; Seow, H.F.; Abdullah, M.; Faisal Jabar, M.; Mohtarrudin, N. Recent updates on mechanisms of resistance to 5-fluorouracil and reversal strategies in colon cancer treatment. *Biology* **2021,** *10,* 854, https://doi.org/10.3390/biology10090854.
25. Sahu, T.; Ratre, Y.K.; Chauhan, S.; Bhaskar, L.V.; Nair, M.P.; Verma, H.K. Nanotechnology based drug delivery system: current strategies and emerging therapeutic potential for medical science. *Journal of Drug Delivery Science and Technology* **2021,** *63,* 102487, https://doi.org/10.1016/j.jddst.2021.102487.
26. Wikantyasning, E.R.; Kalsum, U.; Nurfiani, S.; Da'i, M.; Cholisoh, Z. Allylamine-conjugated polyacrylic acid and gold nanoparticles for colorimetric detection of bacteria. *Materials Science Forum* **2021,** *1029,* 137, https://doi.org/10.4028/www.scientific.net/MSF.1029.137.
27. Sukmawati, A.; Utami, W.; Yuliani, R.; Da'i, M.; Nafarin, A. Effect of tween 80 on nanoparticle preparation of modified chitosan for targeted delivery of combination doxorubicin and curcumin analogue. IOP Conference Series: *Materials Science and Engineering* **2018,** *311,* 012024, https://doi.org/10.1088/1757-899X/311/1/012024.
28. Khan, M.I.; Hossain, M.I.; Hossain, M.K.; Rubel, M.H.; Hossain, K.M.; Mahfuz, A.M.; et al. Recent progress in nanostructured smart drug delivery systems for cancer therapy: a review. *ACS Applied Bio Materials* **2022,** *5,* 971, https://doi.org/10.1021/acsabm.2c00002.
29. Kamel Attar Kar, M.H.; Yousefi, M. Investigating drug delivery of 5-fluorouracil by assistance of an iron-modified graphene scaffold: computational studies. *Main Group Chemistry* **2022,** *21,* 651, https://doi.org/10.3233/MGC-210164.
30. Dhumad, A.M.; Majeed, H.J.; Zandi, H.; Harismah, K. FeC19 cage vehicle for fluorouracil anticancer drug delivery: DFT approach. *Journal of Molecular Liquids* **2021,** *333,* 115905, https://doi.org/10.1016/j.molliq.2021.115905.
31. Yaraghi, A.; Ozkendir, O.M.; Mirzaei, M. DFT studies of 5-fluorouracil tautomers on a silicon graphene nanosheet. *Superlattices and Microstructures* **2015,** *85,* 784, https://doi.org/10.1016/j.spmi.2015.05.053.
32. Liu, Y.; Shah, S.; Tan, J. Computational modeling of nanoparticle targeted drug delivery. *Reviews in Nanoscience and Nanotechnology* **2012,** *1,* 66, https://doi.org/10.1166/rnn.2012.1014.
33. Harismah, K.; Shahrtash, S.A.; Arabi, A.R.; Khadivi, R.; Mirzaei, M.; Akhavan-Sigari, R. Favipiravir attachment to a conical nanocarbon: DFT assessments of the drug delivery approach. *Computational and Theoretical Chemistry* **2022,** *1216,* 113866, https://doi.org/10.1016/j.comptc.2022.113866.
34. Hantoush, A.; Najim, Z.; Abachi, F. Density functional theory, ADME and docking studies of some tetrahydropyrimidine-5-carboxylate derivatives. *Eurasian Chemical Communications* **2022,** *4,* 778, https://doi.org/10.22034/ecc.2022.333898.1374.
35. Ghiasifar, M.; hosseinnejad, T.; Ahangar, A. Copper catalyzed cycloaddition reaction of azidomethyl benzene with 2,2-di(prop-2-yn-1-yl)propane-1,3-diol: DFT and QTAIM investigation. *Progress in Chemical and Biochemical Research* **2022,** *5,* 1, https://doi.org/10.22034/pcbr.2022.319090.1203.
36. Mohamed, H.; Hamza, Z.; Nagdy, A.; El-Mageed, H. Computational studies and DFT calculations of synthesized triazolo pyrimidine derivatives: a review. *Journal of Chemical Reviews* **2022,** *4,* 156, https://doi.org/10.22034/jcr.2022.325439.1138.
37. Moghadam, G.; Ramazani, A.; Zeinali Nasrabadi, F.; Ahankar, H.; Ślepokura, K.; Lis, T.; et al. Single crystal X-ray structure analysis and DFT studies of 3-hydroxyl-1,7,7-trimethyl-3-[5-(4-methylphenyl)-1,3,4-oxadiazol-2-yl]bicycle [2.2.1]heptan-2-one. *Eurasian Chemical Communications* **2022,** *4,* 759, https://doi.org/10.22034/ecc.2022.328320.1320.

38. Chemcraft. https://www.chemcraftprog.com.
39. Frisch, M.J.; Trucks, G.W.; Schlegel, H.B.; Scuseria, G.E.; Robb, M.A.; Cheeseman, J.R.; et al. Gaussian 09 program. *Gaussian Inc.* Wallingford, CT, **2009**, https://gaussian.com.
40. Davidson, E.R.; Chakravorty, S.J. A possible definition of basis set superposition error. *Chemical Physics Letters* **1994,** *217*, 48, https://doi.org/10.1016/0009-2614(93)E1356-L.
41. Bader, R.F.; Matta, C.F. Atomic charges are measurable quantum expectation values: a rebuttal of criticisms of QTAIM charges. *The Journal of Physical Chemistry A* **2004,** *108*, 8385, https://doi.org/10.1021/jp0482666.
42. Lu, T.; Chen, F. Multiwfn: a multifunctional wavefunction analyzer. *Journal of Computational Chemistry* **2012,** *33*, 580, https://doi.org/10.1002/Jcc.22885.
43. Dhahir, Z.; Turkie, N.S. New turbidimetric method for determination of cefotaxime sodium in pharmaceutical drugs using continuous flow injection manifold design with CFTS-vanadium oxide sulfate system. *Chemical Methodologies* **2022,** *6*, 91, https://doi.org/10.22034/chemm.2022.2.2.
44. Mortezagholi, B.; Movahed, E.; Fathi, A.; Soleimani, M.; Forutan Mirhosseini, A.; Zeini, N.; Khatami, M.; Naderifar, M.; Abedi Kiasari, B.; Zareanshahraki, M. Plant-mediated synthesis of silver-doped zinc oxide nanoparticles and evaluation of their antimicrobial activity against bacteria cause tooth decay. *Microscopy Research and Technique* **2022,** *85*, 3553, https://doi.org/10.1002/jemt.24207.
45. Aminian, A.; Fathi, A.; Gerami, M.H.; Arsan, M.; Forutan Mirhosseini, A.; Torabizadeh, S.A. Nanoparticles to overcome bacterial resistance in orthopedic and dental implants. *Nanomedicine Research Journal* **2022,** *7*, 107, https://doi.org/10.22034/nmrj.2022.02.001.
46. Hatami, A.; Heydarinasab, A.; Akbarzadehkhiyavi, A.; Pajoum Shariati, F. An introduction to nanotechnology and drug delivery. *Chemical Methodologies* **2021,** *5*, 153, https://doi.org/10.22034/chemm.2021.121496.
47. Hosseini, S.M.H.; Naimi-Jamal, M.R.; Hassani, M. Preparation and characterization of mebeverine hydrochloride niosomes as controlled release drug delivery system. *Chemical Methodologies* **2022,** *6*, 591, https://doi.org/10.22034/chemm.2022.337717.1482.
48. Tosan, F.; Rahnama, N.; Sakhaei, D.; Fathi, A.H.; Yari, A. Effects of doping metal nanoparticles in hydroxyapatite in Improving the physical and chemical properties of dental implants. *Nanomedicine Research Journal* **2021,** *6*, 327, https://doi.org/10.22034/nmrj.2021.04.002.
49. Saliminasab, M.; Jabbari, H.; Farahmand, H.; Asadi, M.; Soleimani, M.; Fathi, A. Study of antibacterial performance of synthesized silver nanoparticles on Streptococcus mutans bacteria. *Nanomedicine Research Journal* **2022,** *7*, 391, https://doi.org/10.22034/nmrj.2022.04.010.
50. Tallapaneni, V.; Mude, L.; Pamu, D.; Karri, V.V.S.R. Formulation, characterization and in vitro evaluation of dual-drug loaded biomimetic chitosan-collagen hybrid nanocomposite scaffolds. *Journal of Medicinal and Chemical Sciences* **2022,** *5*, 1059, https://doi.org/10.26655/JMCHEMSCI.2022.6.19.